

**NASA TECHNICAL  
MEMORANDUM**



**NASA TM X-3414**

**NASA TM X-3414**

**CASE FILE  
COPY**

**ANALYSIS OF A SOLAR COLLECTOR  
FIELD WATER FLOW NETWORK**

*John E. Rohde and Richard H. Knoll*

*Lewis Research Center*

*Cleveland, Ohio 44135*



|   |  |   |  |  |  |
|---|--|---|--|--|--|
| 1. Report No.<br><b>NASA TM X-3414</b>  |  | 2. Government Accession No.                                 |  | 3. Recipient's Catalog No.   |  |
| 4. Title and Subtitle <b>ANALYSIS OF A SOLAR COLLECTOR FIELD<br/>WATER FLOW NETWORK</b>   |  |   |  | 5. Report Date<br><b>August 1976</b>                                 |  |
|   |  |   |  | 6. Performing Organization Code                                      |  |
| 7. Author(s)<br><b>John E. Rohde and Richard H. Knoll</b>   |  |   |  | 8. Performing Organization Report No.<br><b>E-8709</b>               |  |
|   |  |   |  | 10. Work Unit No.<br><b>776-22</b>                                   |  |
| 9. Performing Organization Name and Address<br><b>Lewis Research Center<br/>National Aeronautics and Space Administration<br/>Cleveland, Ohio 44135</b>   |  |   |  | 11. Contract or Grant No.  |  |
|   |  |   |  | 13. Type of Report and Period Covered<br><b>Technical Memorandum</b> |  |
| 12. Sponsoring Agency Name and Address<br><b>National Aeronautics and Space Administration<br/>Washington, D.C. 20546</b>   |  |   |  | 14. Sponsoring Agency Code   |  |
|   |  |   |  |  |  |
| 15. Supplementary Notes   |  |   |  |  |  |
| 16. Abstract<br><br><p>A number of methods are presented for minimizing the water flow variation in the solar collector field for the Solar Building Test Facility at the Langley Research Center. The solar collector field investigated consisted of collector panels connected in parallel between inlet and exit collector manifolds to form 12 rows. The rows were in turn connected in parallel between the main inlet and exit field manifolds to complete the field. The various solutions considered included various size manifolds, manifold area change, different locations for the inlets and exits to the manifolds, and orifices or flow control valves. Calculations showed that flow variations of less than 5 percent were obtainable both inside a row between solar collector panels and between various rows.</p> |  |   |  |  |  |
| 17. Key Words (Suggested by Author(s))<br><b>Incompressible flow; Solar collector panels;<br/>Flow control; Solar collector field; Flow<br/>network; Solar Building Test Facility</b>   |  |   | 18. Distribution Statement<br><b>Unclassified - unlimited<br/>STAR Category 44</b> |  |  |
| 19. Security Classif. (of this report)<br><b>Unclassified</b>   |  | 20. Security Classif. (of this page)<br><b>Unclassified</b> |  | 21. No. of Pages<br><b>28</b>  |  |
|   |  |   |  | 22. Price*<br><b>\$4.00</b>  |  |

# ANALYSIS OF A SOLAR COLLECTOR FIELD WATER FLOW NETWORK

by John E. Rohde and Richard H. Knoll

Lewis Research Center

## SUMMARY

A number of methods are presented for minimizing the water flow variation caused by the manifolding scheme to be utilized in the solar collector field for the Solar Building Test Facility at the Langley Research Center. The solar collector field investigated consisted of collector panels connected in parallel between inlet and exit collector manifolds to form 12 rows. The rows were in turn connected in parallel between the main inlet and exit field manifolds to complete the field. A number of possible flow solutions are presented both for the variation of flow inside a collector row from collector panel to collector panel and for the variation of flow between collector rows. The various methods of flow control which were considered included various size manifolds, manifold area changes, different locations of the inlets and exits to the manifolds, and orifices or flow control valves. The method ultimately selected was predicated on low initial cost and utilized the minimum size manifolds with fixed orifices for the individual collector panels and flow control valves for the individual collector rows. Calculations showed that flow variations of less than 5 percent were obtainable both inside a row between collector panels and inside the field between collector rows. However, orifices or flow control valves provided balanced flows at only one design flow rate and penalized the overall field efficiency.

## INTRODUCTION

Knowledge of the flow distribution caused by the manifolding in solar collector fields and methods of controlling the flow distribution are required to maximize overall efficiency and performance of a solar collector field. The NASA Lewis Research Center and the NASA Langley Research Center are involved in a joint project to pro-

vide a solar heating and cooling facility for a 4924-square-meter (53 000-sq-ft) single-story office building located at the Langley Research Center in Hampton, Virginia (see ref. 1). The facility will be used to compare the efficiency of various solar collector panels and to serve as a test bed for elements of solar heating and cooling systems. The system will initially provide approximately three-fourths of the total heating and cooling energy required for the office building.

The facility has a nominally 1399-square-meter (15 000-sq-ft) solar collector field located adjacent to the office building. The water flow system for the solar collector field was originally conceived and sized by personnel of the Langley Research Center. Project funding limits and the fact that the field had been conceived and sized before the start of this study somewhat limited the range of alternative designs which were considered. The solar collector field investigated consisted of nominally 51 collector panels connected in parallel between inlet and exit collector manifolds to form one row. Twelve such rows were in turn connected in parallel between the main inlet and exit field manifolds to complete the field. A relatively uniform flow distribution within the field is desired to (1) evaluate properly the performance of the collector panels, (2) maximize the energy output of the field, (3) minimize possible control system problems, and (4) minimize the problems involved in detecting and preventing freezing of the treated water coolant (which contains no antifreeze) during cold weather spells. Collector panel efficiency is dependent both on the flow rate and on the collector panel operating temperature. Lower flow rates will cause the collector panel to run hotter than normal (lose more heat to the surroundings) and thus run at lower efficiency. Also, under night-time freezing conditions collector panels with the lower flow rates could freeze before freezing is indicated by the average fluid temperature.

The investigation described in this report dealt with both the flow variation inside a row from collector panel to collector panel and the overall field flow variation from row to row. Various factors which influence these flow distributions were investigated. These factors include various size manifolds, area change along the manifold, different locations of the inlets and exits to the manifolds, and orifices or flow control valves. The various concepts for flow control presented in this report were jointly proposed by Langley and Lewis personnel, and detailed analysis and calculations were performed by Lewis personnel.

All calculations were made by using the U.S. customary system of units, shown in parentheses.

## DESCRIPTION OF SOLAR COLLECTOR FIELD AND ASSUMPTIONS

The solar collector field for the Solar Building Test Facility has a water flow system which consists of 12 solar collector rows connected in parallel as shown in figure 1. In turn, each solar collector row has a water flow system consisting of a maximum of 51 solar collector panels connected in parallel as shown in figure 2. The following initial dimensions, flow rates, assumptions, and constraints were utilized in the analysis:

- (1) A water flow rate of 2271 to 22 712 cubic centimeters per second (36 to 360 gal/min) for the field
- (2) A water pressure of approximately 69 newtons per square centimeter (100 psia)
- (3) A water temperature of 294 to 366 K (70<sup>0</sup> to 200<sup>0</sup> F)
- (4) An existing inlet and exit field manifold diameter of 10.226 centimeters (4.026 in.) (schedule 40 pipe) (see fig. 1)
- (5) An existing inlet and exit collector manifold diameter of 4.089 centimeters (1.610 in.) (schedule 40 pipe) (see fig. 1)
- (6) A collector panel maximum flow resistance of 0.17 newton per square centimeter (0.25 psi) for a flow of 31.5 cubic centimeters per second (0.5 gal/min) at 366 K (200<sup>0</sup> F)
- (7) A collector panel minimum flow resistance of 0.07 newton per square centimeter (0.10 psi) for a flow of 31.5 cubic centimeters per second (0.5 gal/min) at 366 K (200<sup>0</sup> F)
- (8) Turbulent and one-phase flow in the collector panels
- (9) Standard water properties instead of those of the treated water actually supplied to the solar collector panels (1000 ppm of chromates)

## FLUID FLOW EQUATIONS

Water pressure changes in the field can be attributed to manifold friction pressure losses, manifold momentum pressure changes, orifice flow control pressure losses, and collector panel pressure losses. The frictional pressure drop was calculated from

$$\Delta p_f = \frac{2 \left( \frac{W}{A} \right)^2 f \Delta X}{\rho D_p g}$$

Symbols are defined in the appendix. Friction factors for smooth tubes were determined from the following equations from reference 2:

$$f = \frac{16}{Re} \quad Re < 2300$$

$$\frac{1.0}{\sqrt{f}} = 4.0 \log (Re \sqrt{f}) - 0.40 \quad Re \geq 2300$$

The momentum pressure changes were calculated from

$$\Delta p_m = \frac{(V_e^2 - V_i^2) \rho}{2g}$$

Flow through an orifice was obtained from

$$W = A_{or} K \sqrt{2g \Delta p \rho}$$

which, when written as

$$\Delta p = \frac{\rho V_{or}^2}{2gK^2}$$

gave the desired orifice pressure loss. The orifice discharge coefficients were determined from the following equations taken from reference 3 for a sharp-edged orifice with pipe taps:

$$K = K_o \left( 1 + \frac{\beta C}{Re_p} \right)$$

$$K_o = \frac{10^6 D_{or} K_e}{10^6 D_{or} + 15C}$$

$$K_e = 0.5925 + \frac{0.0182}{D_p} + \left( 0.440 - \frac{0.06}{D_p} \right) \beta^2 + \left( 0.935 + \frac{0.225}{D_p} \right) \beta^5$$

$$+ 1.35 \beta^{14} + \frac{1.43 (0.25 - \beta)^{2.5}}{\sqrt{D_p}}$$

$$C = D_{or} \left( 905 - 5000 \beta + 9000 \beta^2 - 4200 \beta^3 + \frac{875}{D_p} \right)$$

In the equation for  $K_e$ , the last term was dropped when  $\beta > 0.25$ .

The collector panel pressure drop was determined from the following equation, which assumes high Reynolds number turbulent flow inside the collector panel:

$$W_{coll} = R_{coll} \sqrt{\rho \Delta p} \quad (1a)$$

For laminar flow through the collector panels the following equation would apply:

$$W_{coll} = \frac{R_{coll} \rho \Delta p}{\mu} \quad (1b)$$

Note that the viscosity appears in the laminar flow equation and not in the turbulent flow equation. This means that with laminar flow, the water flow rate is a function of water temperature. However, for turbulent flow the water flow rate is not a function of water temperature for the higher Reynolds numbers. For the lower Reynolds number turbulent flow, a secondary effect of viscosity exists. Turbulent flow was assumed in this study except for one case where laminar flow was assumed for purposes of comparison.

The overall pressure drop for a collector row was determined from the following equation, which assumes high Reynolds number turbulent flow inside the field:

$$W_{row} = R_{row} \sqrt{\rho \Delta p} \quad (2)$$

The resulting flow coefficients for the collector panel and row  $R_{coll}$  and  $R_{row}$  were evaluated at their respective design flow rates by using equations (1a) or (1b) and (2). The collector panel flow coefficient  $R_{coll}$  was determined from the maximum or minimum flow resistances, given in the section DESCRIPTION OF SOLAR COLLECTOR FIELD AND ASSUMPTIONS, and checked against experimental data. Information obtained from a detailed analysis of the flow through one row of collector panels over a range of flow rates was required to evaluate the row flow coefficient  $R_{row}$ .

Some care should be exercised when extrapolating the flow coefficients  $R_{coll}$  and  $R_{row}$  to much higher or lower flow rates. Since flow in the collector panels and in the manifolds could be laminar or turbulent, the friction factor varies with Reynolds number, and the inlet and exit losses may follow different relationships.

## NETWORK ANALYSIS

The equations given in the previous section were incorporated into a computer program which solved for the flow distribution in the network. The program was started by specifying the inlet and exit pressures and assuming a flow rate through each collector panel in a given row. The flow rates at all points in the collector manifolds could be determined by using these assumed collector flow rates. With the inlet or exit pressure and the flow distribution in the manifolds known, the pressure distribution in each manifold could be determined. Once the pressure distribution had been obtained in each manifold, a corrected flow rate through each collector panel could be determined. This calculated collector panel flow rate was compared with the initial assumed collector panel flow rate. This procedure was iterated on collector panel flow rate by using the following equation to underrelax the collector panel flow rate values:

$$W_3 = W_1 + (W_2 - W_1)h \quad 0 < h < 2$$

In most cases, values of  $h$  between 0.3 and 0.5 gave convergence after a few iterations. However, under certain conditions the iteration procedure had a tendency to be unstable, and values of  $h$  less than 0.05 were necessary to ensure convergence.

This procedure describes the network analysis of the flow inside a collector row. The overall field network was analyzed in the same way, but the collector row flow rates were assumed instead of the collector panel flow rates. These collector row flow rates and the inlet and exit pressures were used to determine the pressure distribution in the field manifolds. This pressure distribution was used to determine the collector row flow rates, which were then iterated in the same manner as the collector panel flow rates.

## RESULTS AND DISCUSSION

This discussion deals first with the variation of flow inside a collector row from collector panel to collector panel and second with the variation of flow between solar collector rows throughout the field.



## Variations In a Single Collector Row

The network analysis lumps the flow through three collector panels into one equivalent element, with 17 such elements making up a collector row. Finer definition of the flow distribution is not warranted. Figure 2 illustrates two types of feed systems for one row of collector panels. Figure 2(a) illustrates the existing end feed system with the inlet and exit at opposite ends of the collector row. Figure 2(b) illustrates an alternative center feed system which feeds water into and removes water from the center of each collector row.

The flow distribution for the end feed system with 4.080-centimeter-(1.610-in.-) diameter collector manifolds is shown in figure 3 for two collector row flow rates and two pressure drops. The flow rates and pressure drops shown are the basic solar collector field constraints discussed previously. Figures 3(a) and (b) show large variations in the collector panel flow rates at, respectively, the design total collector row flow rate of approximately 1893 cubic centimeters per second (30 gal/min) and the minimum total collector row flow rate of approximately 189 cubic centimeters per second (3 gal/min). The case numbers given in figure 3 refer to the data presented in table I. Table I gives the total row flow rate, overall pressure drop, and geometry of the row for all the cases run. Flow variations are discussed in this report in terms of maximum variation defined by

$$MV = \frac{100(W_{\max} - W_{\min})}{W_{\min}}$$

At the collector row design flow rate the maximum variations are 130 percent for the high-pressure-drop collector panels and 438 percent for the low-pressure-drop collector panels. The variations increase to 242 and 991 percent, respectively, for the high- and low-pressure-drop collectors at the minimum collector row flow condition.

The flow variation predicted for cases 1 and 2 is the result of the size of the collector manifolds which are connected to the collector panels. Figure 4 illustrates the distribution of pressure that exists in the 4.089-centimeter-(1.610-in.-) diameter inlet and exit manifolds. The pressure distribution is affected by momentum pressure increases and decreases and frictional pressure losses, with the latter being the most significant. Frictional losses are high in the sections of the manifolds which flow large quantities of water, and conversely, they are low in the sections of the

manifolds which flow small quantities of water. This pressure distribution causes the flow distribution shown in figure 3(a). Larger manifolds would have more uniform pressure along their length, and consequently there would be a uniform collector flow.

Another factor affecting the flow distribution is whether the water flow through the collector panel is turbulent or laminar. The difference in flow distribution between turbulent and laminar flow in the collector panels is shown in figure 5. The maximum variation in flow rate increases from 130 percent with the turbulent flow in the collector panels to 441 percent with the laminar flow in the collector panels.

The flow variations shown in figures 3 and 5 are, of course, undesirable from a design point of view since the flow variation would not allow all the collector panels to function at their maximum efficiency. Not only would the efficiency be affected by the significantly higher collector exit temperatures near the center of the rows, but also the variation in outlet temperature across the row could cause valve control problems if there were not substantial mixing. A flow variation of 5 percent, however, is considered acceptable since this is comparable with the expected flow variations between collector panels due to manufacturing tolerances. In order to achieve a more reasonable flow variation, alternative methods of controlling the flow distribution were investigated. Four solutions that were investigated were (1) increase the size of the collector manifolds, (2) change the method of feeding the water to the manifolds, (3) utilize stepped manifolds (a manifold with a change in cross-sectional flow area), and (4) utilize orifices to control the flow.

Increasing the diameter of the collector manifolds results in reduced maximum flow variations, as shown in figure 6. Increasing the manifold diameter from 4.089 to 6.271 centimeters (1.610 to 2.469 in.) decreased the maximum flow variation from 130 to 17 percent (see fig. 3), and further increasing the collector manifold to 10.226 centimeters (4.026 in.) decreased the maximum variation to 1.8 percent. Overall row pressure drop also decreased from 1.45 to 0.24 newton per square centimeter (2.10 to 0.35 psi) as the collector manifold diameter increased from 4.089 to 10.226 centimeters (1.610 to 4.026 in.).

Figure 7 presents a comparison of the originally conceived end feed system with an alternative system which feeds water into and out of the center of the collector manifolds (see fig. 2). This comparison is made for a collector manifold diameter of 6.271 centimeters (2.469 in.) so as to produce realistic flow variations. Figure 7 shows that the center feed system provides a reduced maximum flow variation of

6.1 percent, as compared with 17 percent for the end feed system. Also, the overall row pressure drop (see table I) is lower for the center feed system than for the end feed system, 0.28 newton per square centimeter (0.40 psi), as compared with 0.38 newton per square centimeter (0.55 psi). Therefore, less pressure drop is required to obtain the improved flow distribution with the center feed system. Results are also shown in table I for a center feed configuration, case 9, with the collector manifold diameter increased to 7.793 centimeters (3.068 in.). This larger collector manifold diameter results in an acceptable maximum flow variation of 2.2 percent.

Figure 8 presents the geometry of two stepped manifold configurations which were investigated. Obviously, there are a large number of possible step combinations which could be considered, and no attempt was made to reach an optimum configuration. Figure 9 shows a very erratic but overall uniform flow rate for these stepped manifolds. The end feed stepped manifold has a maximum variation of 4.0 percent, and the center feed stepped manifold has a maximum variation of 4.2 percent.

The last solution, the one finally selected on the basis of lowest initial system cost, utilized sharp-edged orifices in series with the collector panels to throttle the flow through the higher flow panels of the end feed system. The smaller collector manifold diameter of 4.089 centimeters (1.610 in.) was maintained. Table II presents the sharp-edged orifice sizes which are required in series with the collector panels that have turbulent flow through them. The orifice size variations are limited to standard drill sizes to facilitate manufacturing. These standard size orifices result in some flow variations at the design collector flow rate of 1893 cubic centimeters per second (30 gal/min) with the most sensitive collector panels being the ones with the lowest pressure drop. These low-pressure-drop collector panels are the most sensitive to the manifold pressure distribution. Figure 10 shows the calculated flow variation at the collector row design flow rate. Maximum variations range from 2.2 to 3.4 percent for the high- and low-pressure-drop collectors, respectively, values which are well within the goal of 5 percent.

The tradeoff involved in selecting the smaller diameter manifold with orifices over the other solutions (larger manifolds, stepped manifolds, and center feed) is primarily that of initial system cost. The more desirable solutions from an efficiency standpoint all require larger more expensive piping. The center feed with orifices

could be used, but other project considerations preclude this.

Although the initial cost is lower, there are disadvantages to the orifice solution. First, more pumping power is required. For example, as shown in table I, the overall collector row pressure drop increases from 0.24 newton per square centimeter (0.35 psi) for the 10.226-centimeter (4.026-in.) collector manifolds to 1.69 newtons per square centimeter (2.45 psi) for the 4.089-centimeter (1.610-in.) collector manifolds with orifices on 45 of the 51 collector panels in the row. The additional pumping power, of course, increases operating costs. Second, operating with flow rates significantly lower than design flow (down to 10 percent) can cause larger variations in the flow distribution. As shown in figure 11, at the minimum collector row flow rate of 189 cubic centimeters per second (3 gal/min) the orifices do not provide balanced flows. The maximum flow variations are 40 and 69 percent for the high- and low-pressure-drop collectors, respectively, at the minimum collector row flow rate. These values compare with 2.2 and 3.4 percent for the corresponding design collector row flow rate.

Figure 12 shows the maximum variation in flow rate between panels with the lowest pressure drop over the range of collector row flow rates for the solution with orifices. Also shown for reference is the solution with the collector manifold diameter increased to 10.226 centimeters (4.026 in.) without orifices. The solution with the smaller manifold and the orifices shows the large flow variation at the low flow rate (10 percent of design), but the variation drops off quite rapidly as the flow rate increases. For example, at 20 percent of the design flow the maximum flow variation drops off to 35 percent compared with 69 percent at the lower flow. For the larger diameter manifold without orifices, the 10.226-centimeter (4.026-in.) manifold, the maximum flow variation remains below 10 percent for the flows examined.

### Variations in Overall Solar Collector Field

This section considers the variation of flow between the 12 rows of solar collectors shown in figure 1. The collector row overall pressure drop was determined from the analysis of the flow through a row of collector panels at the design point. (See the section FLUID FLOW EQUATIONS.) Table III gives the overall total field flow rate, overall field pressure drop, and geometry for the cases analyzed.

The flow distribution for the existing field with 10.226-centimeter (4.026-in.)

field manifolds and 4.089-centimeter (1.610-in.) collector manifolds with orifices added (case 16, table III) is shown in figure 13. The maximum flow variation is 38 percent between the flow in row 1 and row 11. This flow variation between rows is in addition to the previously discussed 2.2-percent variation with orifices which exists inside the rows from collector panel to collector panel (as shown in fig. 10). The flow variation shown in figure 13 is caused by the water pressure distribution that exists in the field manifolds. Figure 14 gives that water pressure distribution. The pressure distribution is the result of frictional losses and momentum pressure increases and decreases. Note that the small-diameter collector manifold utilized results in a relative large pressure drop across the collector row. This can be seen by comparing the pressure loss over the length of the exit or inlet field manifold with the collector row pressure drop across any row. This relatively large collector row pressure drop attenuates the pressure variation in the row manifolds and thus produces the modest variation of 38 percent.

Although modest, this variation is probably not an acceptable flow variation when the field is to be used as a research facility to compare the performance of different solar collector panel designs in each row. To give a realistic comparison, each collector row should be provided with the same pressure drop between the field manifolds and a fixed outlet water temperature level. This flow variation could be controlled by orifices or flow control valves to adjust the pressure drop across the row, increased manifold diameter, stepped manifolds, or a center feed system. Installing 12 flow control valves is the approach that was taken, since these same valves are required for maintenance. Adding flow control valves in each row in the field, cases 22 and 23, provides uniform flow but increases the overall pressure drop to 3.61 and 3.36 newtons per square centimeter (5.24 and 4.88 psi), respectively, for the existing manifolds with and without orifices in series with the collector panels (see table III.) The addition of flow control valves increased the pressure loss 0.51 newton per square centimeter (0.74 psi) (case 23 compared with case 16). It should be noted that the flow control valve setting matches the flow at only one flow rate condition. However, unlike the orifices, these flow control valves allow the rows to be balanced, if necessary, at other conditions by changing the settings. The maximum variation between rows with the flow control valves wide open would be the 38 percent shown in figure 13.

An improved collector panel field geometry from the standpoint of overall system

efficiency was determined by assuming that an end feed system (see fig. 2(a)) with 10.226-centimeter (4.026-in.) collector manifolds would be utilized. This system provides the smallest flow variation (e.g., see fig. 6) and the least physical change to the field geometry. This geometry for the collector manifolds and various diameters for the inlet and exit field manifolds were used to obtain the flow variations shown in figure 15. This figure shows that the field manifold diameter must be increased to 25.451 centimeters (10.020 in.) in order to reduce the flow variation to less than 5 percent.

A comparison of the two cases with 10.226-centimeter-(4.026-in.-) diameter field manifolds (figs. 13 and 15) indicates a large difference in the flow variation. This difference is the result of the fact that the collector row pressure drop is much smaller for the 10.226-centimeter-(4.026-in.-) diameter collector manifolds. This relatively low collector row pressure drop as compared with the pressure drop in the inlet and exit manifolds means that the manifold pressure distribution controls the flow and produces the large flow variation shown in figure 15.

From the standpoint of overall field efficiency, the variation of 3.1 percent for the 25.451-centimeter-(10.020-in.-) diameter inlet and exit manifolds should be acceptable. However, the maintenance requirements of the experimental field, the cost of the larger pipe sizes throughout the field in conjunction with the larger flow control valves required, and the desirability of minimizing the flow variation dictate the use of flow control valves in each row. It is more desirable to accept the additional pumping power required for the existing field with the orifices, flow control valves, and smaller pipe sizes. However, it should be noted that the overall pressure drop increases from 0.28 newton per square centimeter (0.40 psi) for the larger manifolds to 3.61 newtons per square centimeter (5.24 psi) for the smaller manifolds with orifices in series with the collector panels and flow control valves in the rows. The overall field pumping loss for the addition of orifices and flow control valves amounts to 746 watts (1.0 hp). This loss, of course, must be considered in the overall analysis of system performance.

Although not analyzed, either a stepped manifold or a center feed system would provide some additional improvement in the maximum flow variation between rows.

## CONCLUDING REMARKS

Larger manifold diameters, center feed manifolds, manifolds with varying area, and flow control valves or orifices provide methods of controlling the variation of flow inside a collector row from collector panel to collector panel and also the variation of flow between collector rows. Laminar flow through the collector panel, instead of the assumed turbulent flow, was shown to produce larger flow variations and would therefore require additional control.

The method of balancing the flow that was finally selected for the solar collector field of the Solar Building Test Facility involved using the existing end feed configuration with the small diameter pipes and adding orifices in series with the collector panels and flow control valves in each of the 12 rows. This configuration permits the basic research objectives and functional (or operational) requirements to be met for the lowest initial cost. Granted, the overall system efficiency suffers because of the additional pressure loss caused by the orifices and flow control valves, but for a research system the additional pump and orifices are cheaper than the cost of purchasing the large diameter pipe for all the manifolds involved. The only minor problem with this system will be the slight flow variation between collector panels at off-design flow rates.

For each collector row (total of 12 rows in the field), 45 of the 51 collector panels will require an orifice in series with the collector panel. The orifices for the individual collector panels have been sized for the design flow rate over the range of pressure drops anticipated. At the design flow rate of 1893 cubic centimeters per second (30 gal/min) the flow variation within a collector row will be less than 5 percent. At one-tenth the design flow rate, which is likely to be encountered during daily startup and shutdown, the maximum variation could reach 69 percent.

The maximum flow variation between rows will be 38 percent with the flow control valves wide open. This variation, however, can be reduced to zero by adjusting the 12 individual row flow control valves. Besides enabling uniform test conditions for individual rows, the flow control valves will facilitate the operation and maintenance of the solar collector field.

Lewis Research Center,

National Aeronautics and Space Administration,

Cleveland, Ohio, April 22, 1976,

776-22.

## APPENDIX – SYMBOLS

|         |  |
|---------|--|
| A       | flow area                                  |
| C       | orifice discharge coefficient term         |
| D       | hydraulic diameter                         |
| f       | friction factor                            |
| g       | gravitational conversion factor            |
| h       | relaxation factor                          |
| K       | orifice discharge coefficient              |
| $K_e$   | orifice discharge coefficient term         |
| $K_o$   | orifice discharge coefficient term         |
| MV      | maximum variation in flow rate             |
| p       | pressure                                   |
| R       | flow coefficient                           |
| Re      | Reynolds number                            |
| V       | velocity                                   |
| W       | mass weight of flow                        |
| X       | linear distance along passage              |
| $\beta$ | ratio of orifice diameter to pipe diameter |
| $\mu$   | dynamic viscosity                          |
| $\rho$  | density                                    |

### Subscripts:

|      |                 |
|------|-----------------|
| coll | collector panel |
| e    | exit            |
| f    | friction        |
| i    | inlet           |
| m    | momentum        |



max    maximum

min    minimum

or      orifice

p       pipe

row    row

1       first iteration

2       second iteration

3       third iteration

## REFERENCES

1. Ragsdale, Robert G.; and Namkoong, David: The NASA Langley Building Solar Project and the Supporting Lewis Solar Technology Program. NASA TM X-71600, 1974.
2. McAdams, William H.: Heat Transmission. 3rd ed., McGraw-Hill Book Co., Inc., 1954.
3. Fluid Meters, Their Theory and Application. 5th ed., Am. Soc. Mech. Engrs., 1959.

TABLE I. - OVERALL COLLECTOR ROW TOTAL FLOW RATE AND OVERALL ROW PRESSURE DROP  
FOR VARIOUS CONDITIONS

[Water temperature, 366 K (200° F).]

| Case           | Feed system | Collector manifold diameter |       | Base collector panel pressure drop |      | Collector panel orifices<br>(see table II) | Total row flow rate  |         | Overall row pressure drop |      | Maximum row variation, percent |
|----------------|-------------|-----------------------------|-------|------------------------------------|------|--|----------------------|---------|---------------------------|------|--------------------------------|
|                |             | cm                          | in.   | N/cm <sup>2</sup>                  | psi  |  | cm <sup>3</sup> /sec | gal/min | N/cm <sup>2</sup>         | psi  |                                |
| 1              | End         | 4.089                       | 1.610 | 0.17                               | 0.25 | No   | 1867                 | 29.6    | 1.45                      | 2.10 | 130                            |
| 2              | ↓           | ↓                           | ↓     | .07                                | .10  | ↓  | 1912                 | 30.3    | 1.31                      | 1.90 | 438                            |
| 3              | ↓           | ↓                           | ↓     | .17                                | .25  | ↓  | 179                  | 2.84    | .02                       | .03  | 242                            |
| 4              | ↓           | ↓                           | ↓     | .07                                | .10  | ↓  | 255                  | 4.04    | .03                       | .05  | 991                            |
| <sup>a</sup> 5 | ↓           | ↓                           | ↓     | .17                                | .25  | ↓  | 1962                 | 31.1    | 1.45                      | 2.10 | 414                            |
| 6              | ↓           | 6.271                       | 2.469 | ↓                                  | ↓    | ↓  | 1830                 | 29.0    | .38                       | .55  | 17                             |
| 7              | ↓           | 10.226                      | 4.026 | ↓                                  | ↓    | ↓  | 1842                 | 29.2    | .24                       | .35  | 1.8                            |
| 8              | Center      | 6.271                       | 2.469 | ↓                                  | ↓    | ↓  | 1830                 | 29.0    | .28                       | .40  | 6.1                            |
| 9              | Center      | 7.793                       | 3.068 | ↓                                  | ↓    | ↓  | 1830                 | 29.0    | .24                       | .35  | 2.2                            |
| 10             | End         | (b)                         | (b)   | ↓                                  | ↓    | ↓  | 2000                 | 31.7    | .34                       | .50  | 4.0                            |
| 11             | Center      | (c)                         | (c)   | ↓                                  | ↓    | ↓  | 1943                 | 30.8    | .28                       | .40  | 4.2                            |
| 12             | End         | 4.089                       | 1.610 | ↓                                  | ↓    | Yes  | 1867                 | 29.6    | 1.69                      | 2.45 | 2.2                            |
| 13             | ↓           | ↓                           | ↓     | .07                                | .10  | ↓  | 1893                 | 30.0    | 1.59                      | 2.30 | 3.4                            |
| 14             | ↓           | ↓                           | ↓     | .17                                | .25  | ↓  | 182                  | 2.88    | .03                       | .04  | 40                             |
| 15             | ↓           | ↓                           | ↓     | .07                                | .10  | ↓  | 172                  | 2.73    | .02                       | .03  | 69                             |

<sup>a</sup>Laminar water flow in collector panels instead of turbulent flow.

<sup>b</sup>Stepped manifolds (see fig. 8(a)).

<sup>c</sup>Stepped manifolds (see fig. 8(b)).

TABLE II. - SIZE OF SHARP-  
EDGED ORIFICES TO BE  
UTILIZED IN EACH ROW OF  
COLLECTOR PANELS

| Collector panel<br>(see fig. 2) | Orifice diameter |       |
|---------------------------------|------------------|-------|
|                                 | cm               | in.   |
| 1-3                             | 0.505            | 0.199 |
| 4-6                             | .541             | .213  |
| 7-9                             | .579             | .228  |
| 10-12                           | .635             | .250  |
| 13-15                           | .714             | .281  |
| 16-18                           | .820             | .323  |
| 19-21                           | .980             | .386  |
| 22-27                           | (a)              | (a)   |
| 28-30                           | .909             | .358  |
| 31-33                           | .767             | .302  |
| 34-36                           | .676             | .266  |
| 37-39                           | .605             | .238  |
| 40-42                           | .561             | .221  |
| 43-45                           | .518             | .204  |
| 46-48                           | .485             | .191  |
| 49-51                           | .457             | .180  |

<sup>a</sup>No orifices.

TABLE III. - OVERALL FIELD TOTAL FLOW RATE AND OVERALL FIELD PRESSURE DROP  
FOR VARIOUS CONDITIONS

[Base collector panel pressure drop,  $0.17 \text{ N/cm}^2$  (0.25 psi).]

| Case | Collector manifold diameter |       | Collector panel orifices<br>(see table II) | Field manifold diameter |        | Valves on rows | Total field flow rate |         | Overall field pressure drop |      | Maximum field variation, percent |
|------|-----------------------------|-------|--|-------------------------|--------|----------------|-----------------------|---------|-----------------------------|------|----------------------------------|
|      | cm                          | in.   |  | cm                      | in.    |                | cm <sup>3</sup> /sec  | gal/min | N/cm <sup>2</sup>           | psi  |                                  |
| 16   | 4.089                       | 1.610 | Yes  | 10.226                  | 4.026  | No             | 22 586                | 358     | 3.10                        | 4.50 | 38                               |
| 17   | 10.226                      | 4.026 | No   | 10.226                  | 4.026  | ↓              | 22 776                | 361     | 1.45                        | 2.10 | 220                              |
| 18   | ↓                           | ↓     | ↓  | 12.819                  | 5.047  |                | 22 460                | 356     | .69                         | 1.00 | 80                               |
| 19   |                             |       |  | 15.405                  | 6.065  |                | 22 649                | 359     | .45                         | .65  | 35                               |
| 20   |                             |       |  | 20.272                  | 7.981  |                | 22 776                | 361     | .31                         | .45  | 9.6                              |
| 21   |                             |       |  | 25.451                  | 10.020 |                | 22 839                | 362     | .28                         | .40  | 3.1                              |
| 22   | 4.089                       | 1.610 | ↓  | 10.226                  | 4.026  | Yes            | 22 712                | 360     | 3.36                        | 4.88 | 0                                |
| 23   | 4.089                       | 1.610 | Yes  | 10.226                  | 4.026  | Yes            | 22 712                | 360     | 3.61                        | 5.24 | 0                                |

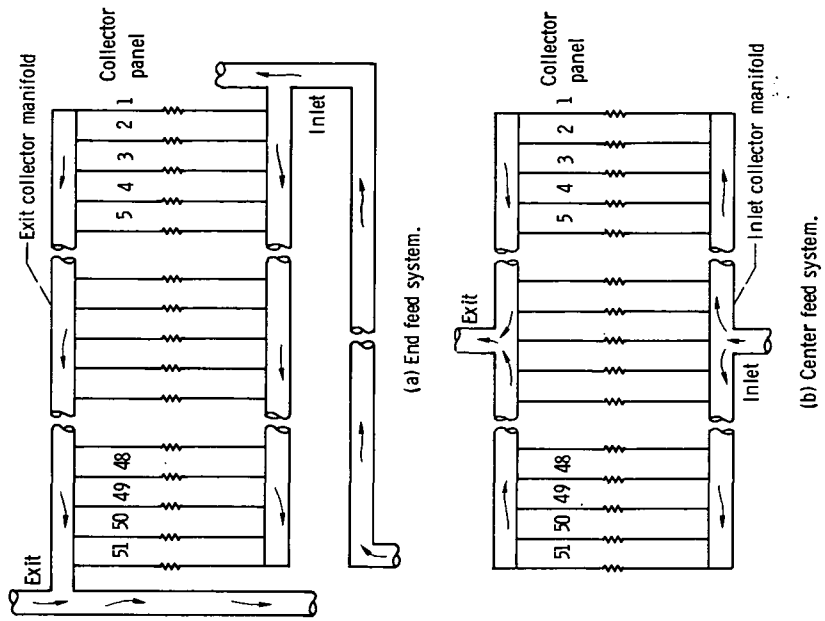


Figure 2. - Feed systems for one row of solar collectors.

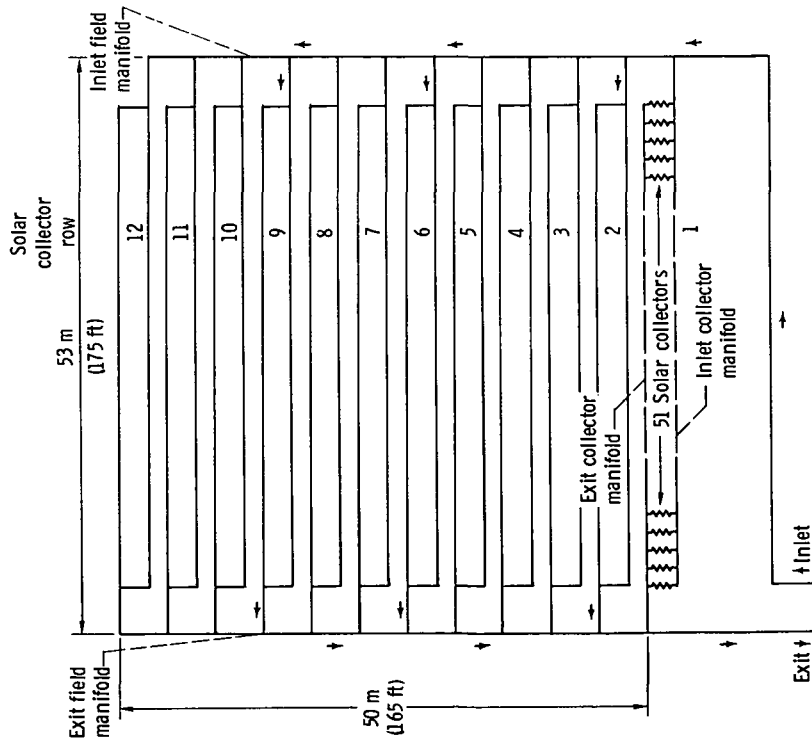


Figure 1. - Solar collector field layout.

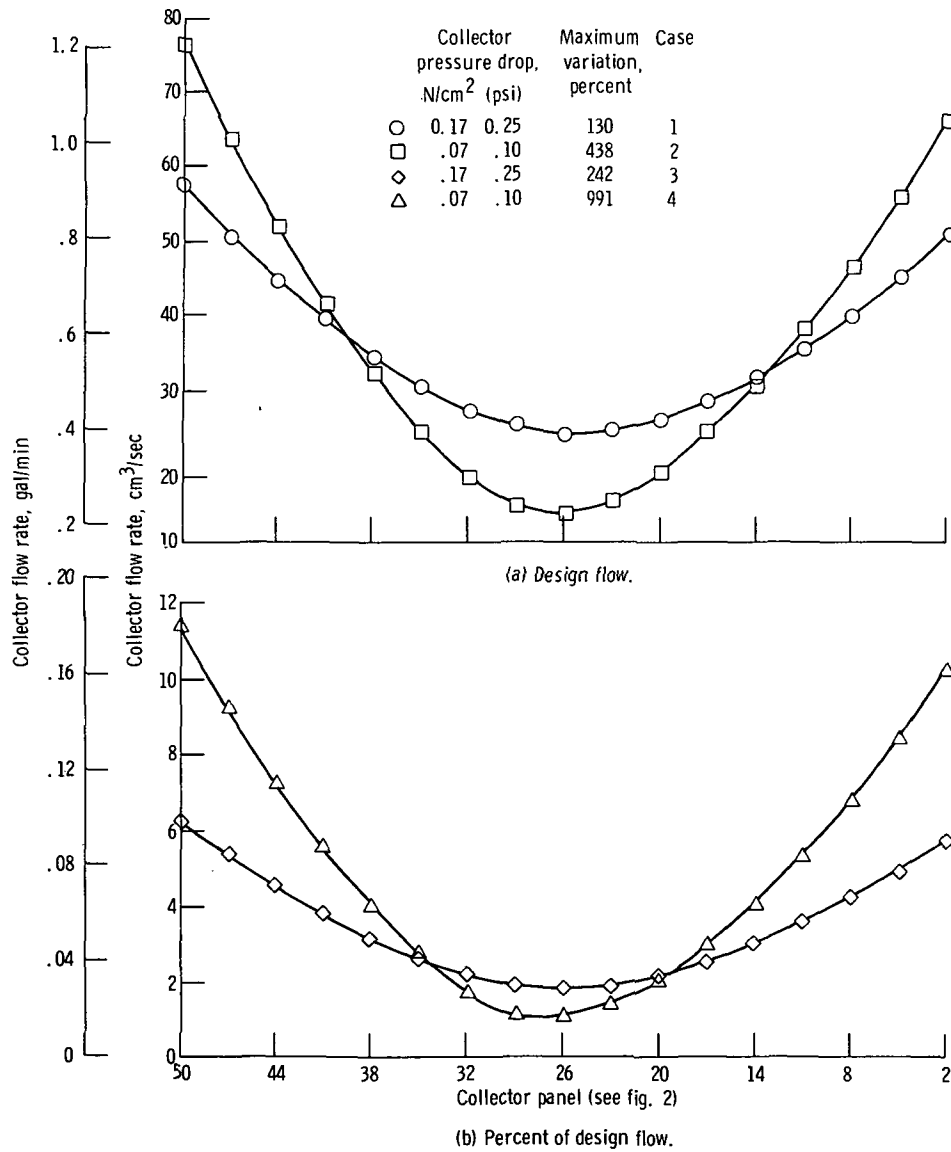


Figure 3. - Flow variation in end feed system with collector manifold diameter of 4,089 centimeters (1.610 in.).

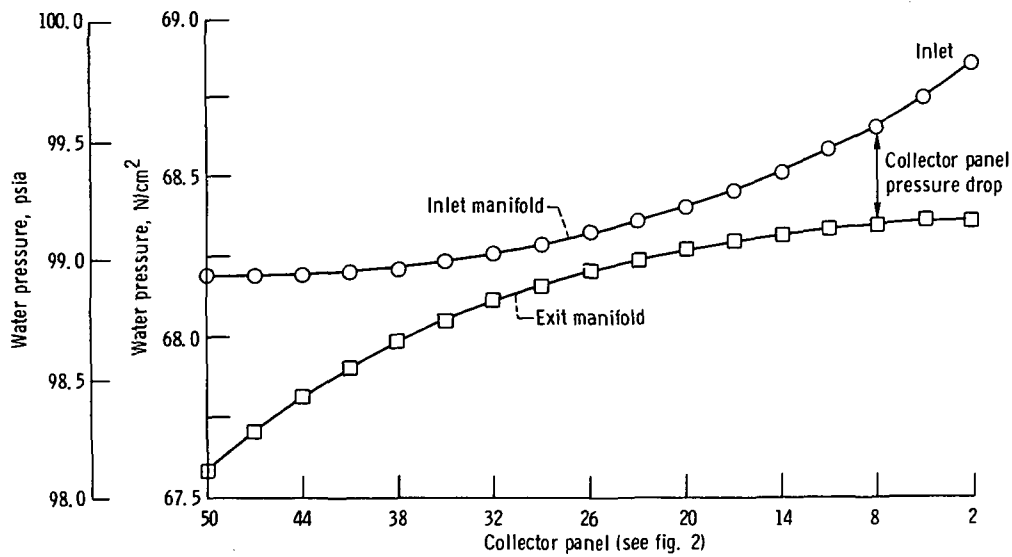


Figure 4. - Water pressure distribution in end feed collector manifolds with inlet and exit collector manifold with inlet and exit collector manifold diameter of 4.089 centimeters (1.610 in.), case 1.

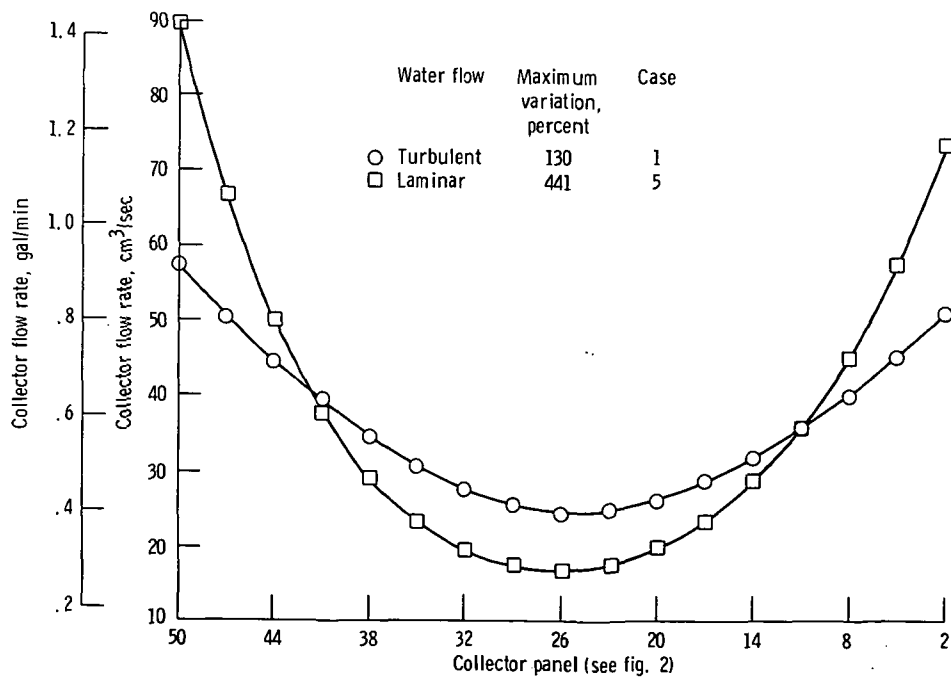


Figure 5. - Flow variation in end feed system with turbulent or laminar water flow through 0.17-newton-per-square-centimeter (0.25-psi-) pressure-drop collector panels.

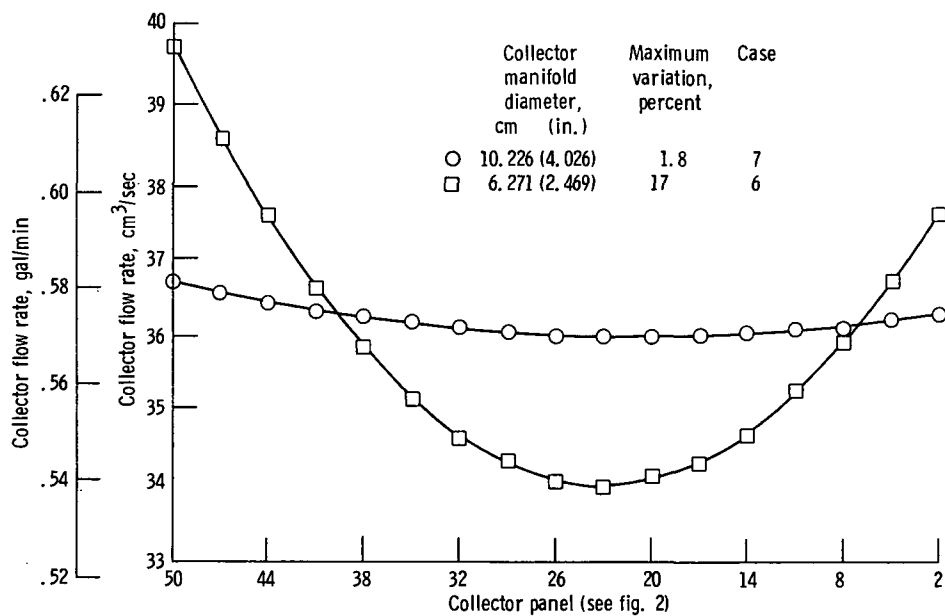


Figure 6. - Flow variation in end feed system with larger diameter collector manifolds and 0.17-newton-per-square-centimeter- (0.25-psi-) pressure-drop collector panels.

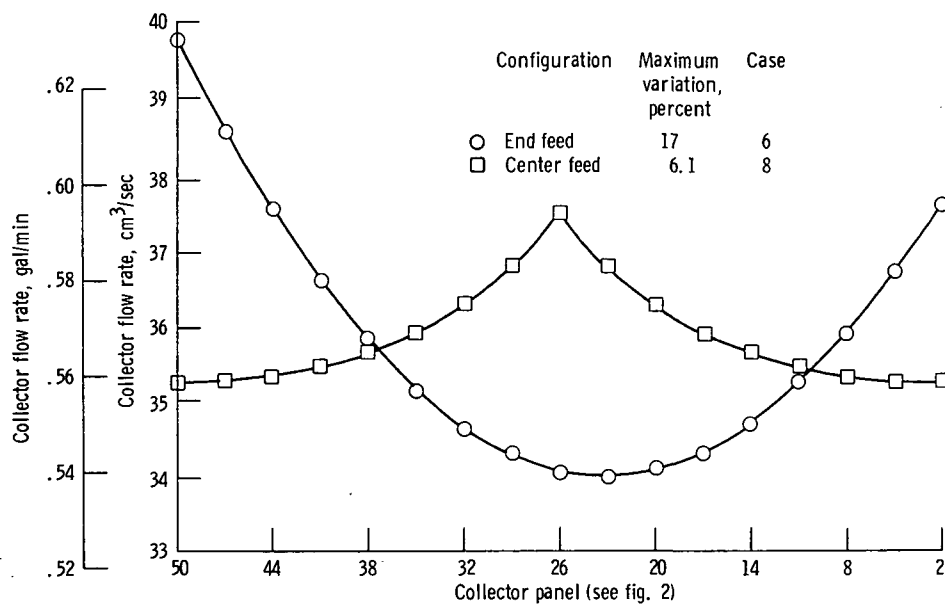
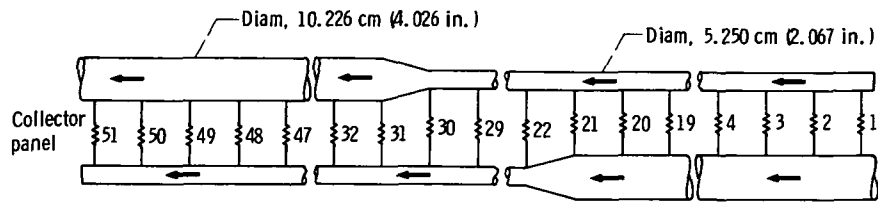
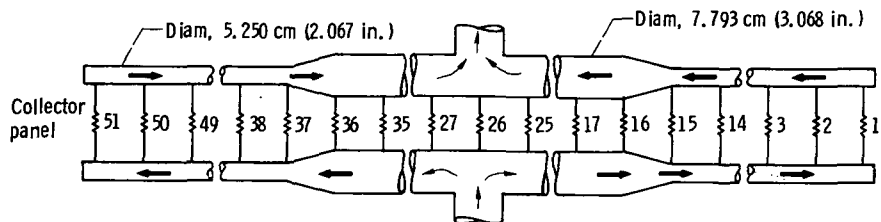


Figure 7. - Flow variation in end and center feed configuration with collector manifold diameter of 6.271 centimeters (2.469 in.) and collector panels having pressure drop of 0.17 newton per square centimeter (0.25 psi).





(a) End feed system.



(b) Center feed system.

Figure 8. - Two stepped manifold configurations for collector row.

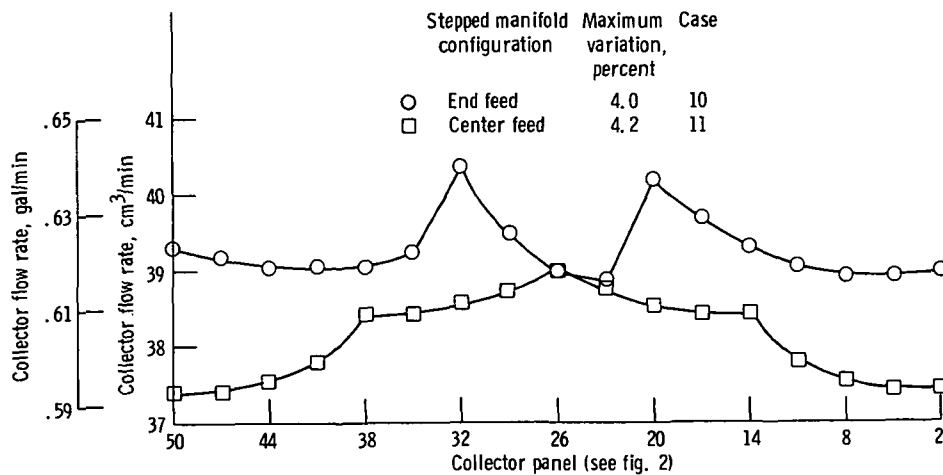


Figure 9. - Flow variation in stepped collector manifolds with 0.17-newton-per-square-centimeter- (0.25-psi) pressure-drop collector panels (see fig. 8).

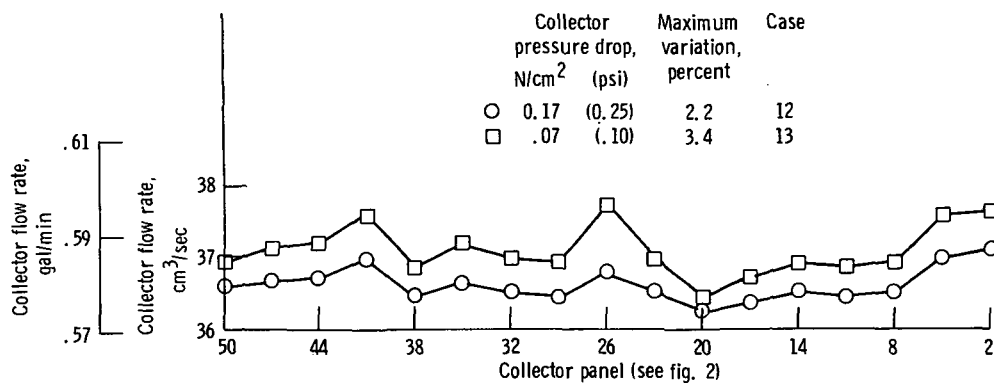


Figure 10. - Flow variation in end feed system with orifices with collector manifold diameter of 4.089 centimeters (1.610 in.) at design flow.

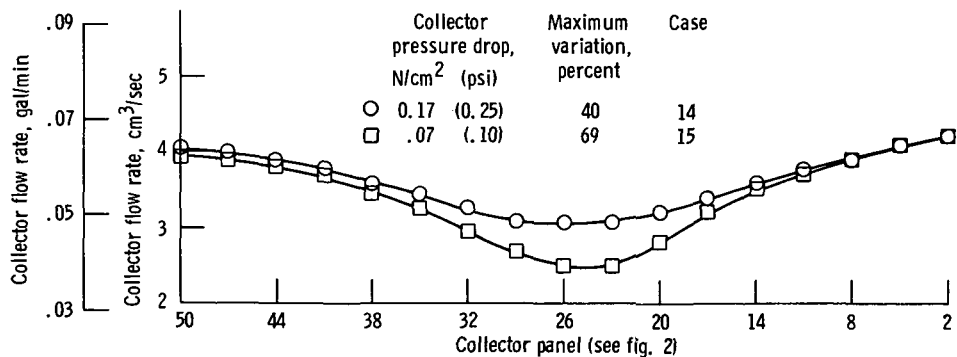


Figure 11. - Flow variation in end feed system with orifices at 10 percent of design flow.

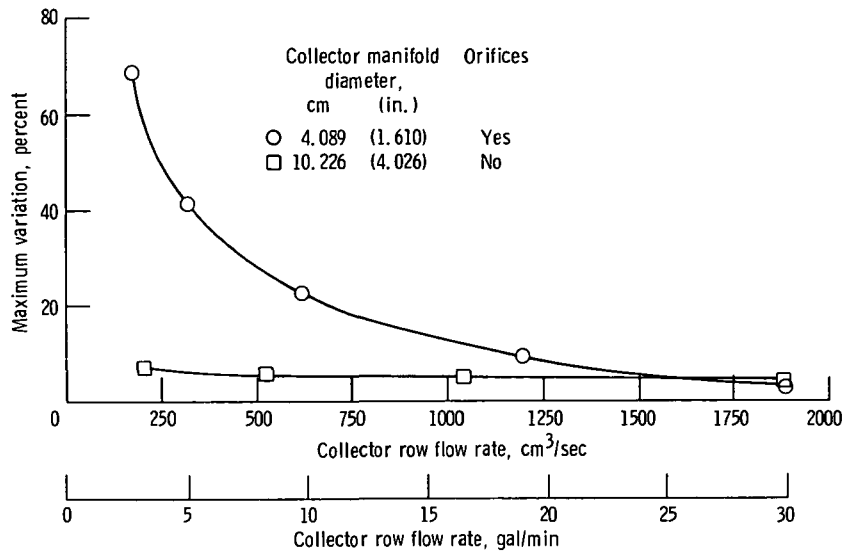


Figure 12. - Maximum percent variation in end feed system for various total flow rates with 0.07-newton-per-square-centimeter- (0.10-psi-) pressure-drop collector panels.

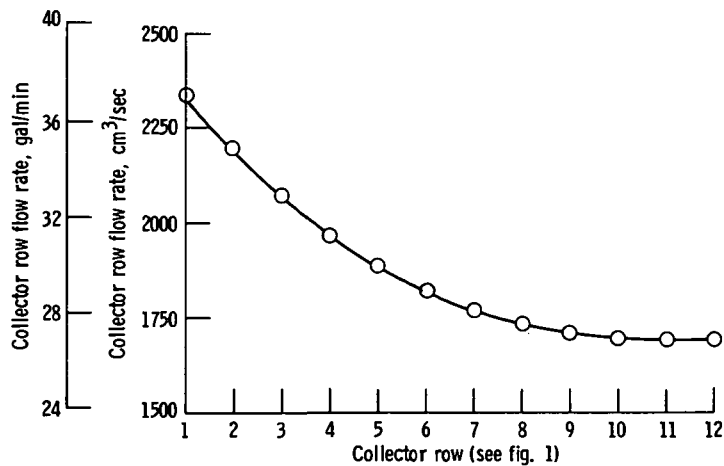


Figure 13. - Flow variation in existing field with orifices on each collector panel and 0.17-newton-per-square-centimeter- (0.25-psi-) pressure-drop collector panels connected by 10.226-centimeter (4.026-in.) field manifolds. Maximum variation, 38 percent; case 16.

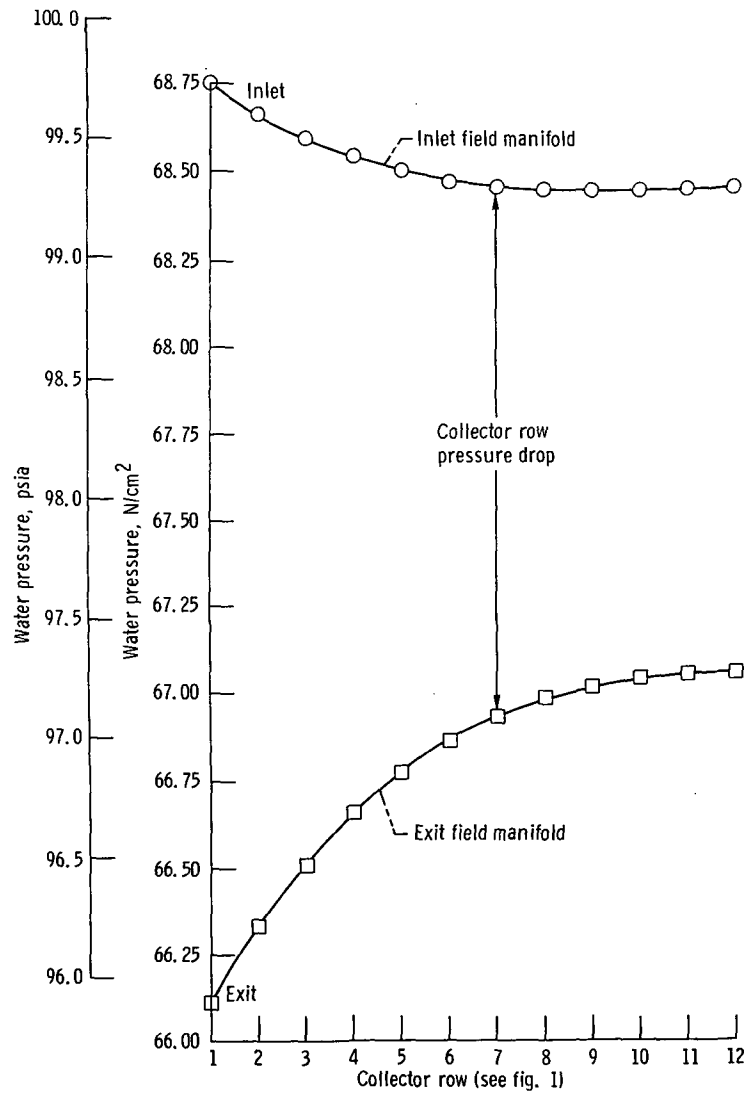


Figure 14. - Water pressure distribution in 10.226-centimeter (4.026-in.) field manifolds of existing field with orifices on each collector panel and 0.17-newton-per-square-centimeter (0.25-psi) pressure-drop collector panels. Case 16.

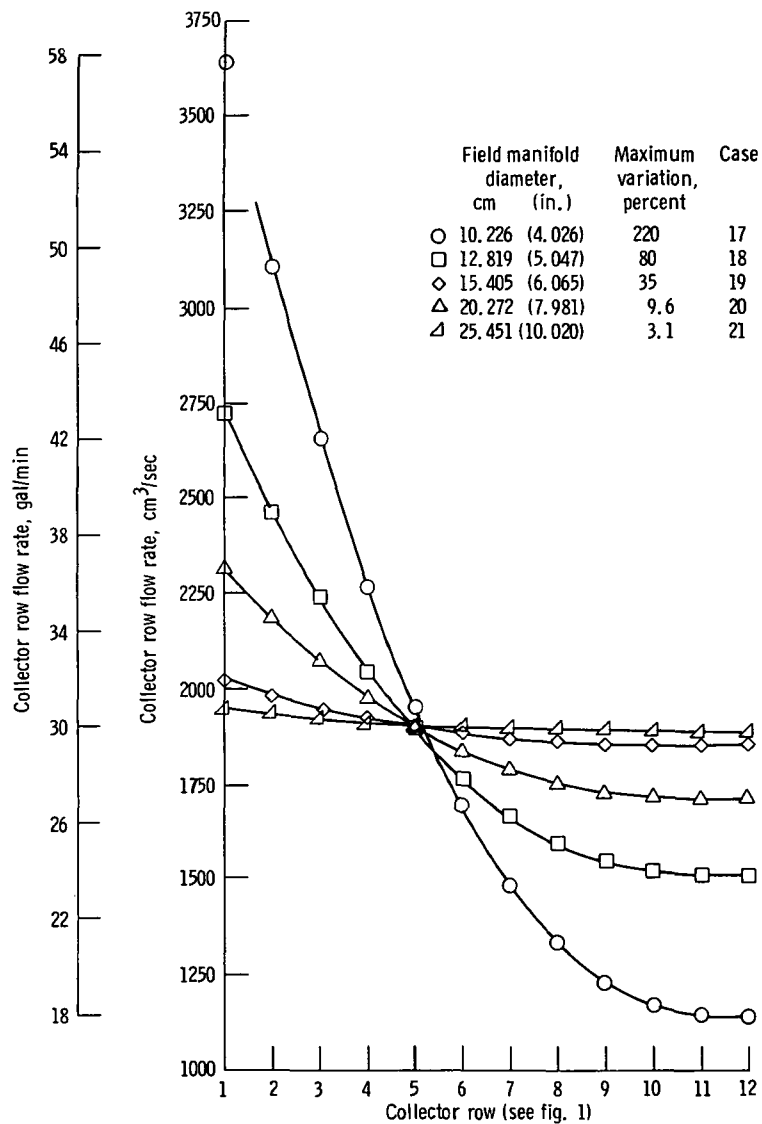


Figure 15. - Flow variation in field for various field manifold diameters with collector manifold diameter of 10.226 centimeters (4.026 in.) and 0.17-newton-per-square-centimeter - (0.25-psi-) pressure-drop collector panels.

NATIONAL AERONAUTICS AND SPACE ADMINISTRATION  
WASHINGTON, D.C. 20546

OFFICIAL BUSINESS  
PENALTY FOR PRIVATE USE \$300

SPECIAL FOURTH-CLASS RATE  
BOOK

POSTAGE AND FEES PAID  
NATIONAL AERONAUTICS AND  
SPACE ADMINISTRATION  
451



POSTMASTER : If Undeliverable (Section 158  
Postal Manual) Do Not Return

*"The aeronautical and space activities of the United States shall be conducted so as to contribute . . . to the expansion of human knowledge of phenomena in the atmosphere and space. The Administration shall provide for the widest practicable and appropriate dissemination of information concerning its activities and the results thereof."*

—NATIONAL AERONAUTICS AND SPACE ACT OF 1958

## NASA SCIENTIFIC AND TECHNICAL PUBLICATIONS

**TECHNICAL REPORTS:** Scientific and technical information considered important, complete, and a lasting contribution to existing knowledge.

**TECHNICAL NOTES:** Information less broad in scope but nevertheless of importance as a contribution to existing knowledge.

**TECHNICAL MEMORANDUMS:** Information receiving limited distribution because of preliminary data, security classification, or other reasons. Also includes conference proceedings with either limited or unlimited distribution.

**CONTRACTOR REPORTS:** Scientific and technical information generated under a NASA contract or grant and considered an important contribution to existing knowledge.

**TECHNICAL TRANSLATIONS:** Information published in a foreign language considered to merit NASA distribution in English.

**SPECIAL PUBLICATIONS:** Information derived from or of value to NASA activities. Publications include final reports of major projects, monographs, data compilations, handbooks, sourcebooks, and special bibliographies.

**TECHNOLOGY UTILIZATION PUBLICATIONS:** Information on technology used by NASA that may be of particular interest in commercial and other non-aerospace applications. Publications include Tech Briefs, Technology Utilization Reports and Technology Surveys.

*Details on the availability of these publications may be obtained from:*

**SCIENTIFIC AND TECHNICAL INFORMATION OFFICE**

**NATIONAL AERONAUTICS AND SPACE ADMINISTRATION**

**Washington, D.C. 20546**